# 3D deformation measuring system for physical modelling in geotechnics.

B. T. LE, S. NADIMI, R.J. GOODEY, R.N. TAYLOR

Abstract: A newly developed imaging system is presented that measures three dimensional deformations of a soil surface in geotechnical experiments involving physical modelling. The method adopts the computer vision technique *Structure from Motion* and *Multi-View Stereo* delivered by an open source software MicMac. Three 2 MegaPixel (MP) industrial cameras were synchronised and used to capture images of a deforming soil surface. The images were used to reconstruct the observed scene to a high density, accurate 3D point cloud. A new method has been developed to process the obtained 3D point clouds and images to determine 3D displacement vectors. The procedure is highly automatic which allows large data sets to be processed with minimal manual intervention. Two series of quantification experiments were carried out to assess the performance of the system which showed the overall accuracy to be within 0.05mm over a field of view of 500×250mm. An example application is presented to demonstrate the capabilities of the 3D imaging system.

**KEYWORDS**: centrifuge modelling; deformation; ground movements; laboratory equipment; laboratory tests; model tests

## INTRODUCTION

Measurement of soil deformation is critical to investigating geotechnical behaviour during physical model studies. Three dimensional experiments can reveal more detail of the soil behaviour which cannot be obtained in two dimensional, plane strain experiments. Conventional instrumentation such as displacement transducers give local movements in one direction and cannot reveal the overall movements of a soil surface. Digital imaging techniques, e.g. Particle Image Velocity (PIV), also termed Digital Image Correlation (DIC) can only measure one and two dimensional soil displacements of a plane surface (White *et al*., 2003, Nadimi *et al*., 2016).

A contactless, image-based measuring system for determining movements of a 3D surface will have obvious benefits to geotechnical physical modelling research. One of the early image analysis systems for determining 3D surface topography of soil models using the close range photogrammetry technique was introduced by Taylor *et al*. (1998). The precision was reported at 57μm, 42μm and 98μm in X, Y and Z directions respectively. The technique relied upon tracking of targets embedded in the surface of soil model.

In this paper, a new method is presented which utilises a 3D point cloud obtained from processed images to determine 3D displacement vectors. The system performance is quantified by a set of experiments and illustrated by a centrifuge modelling example application. The performance of the measurement system is assessed by its accuracy, precision and repeatability. Accuracy is defined as the deviation between the true value and the measured value. Precision is defined as the random

difference between the various measurements of a same value. Repeatability is defined as the consistency of the achieved accuracy and precision under constant measurement conditions.

## PRINCIPLE AND PERFORMANCE

This research uses an open source software MicMac which incorporates Structure from Motion and Multi-View Stereo (SfM-MVS) techniques.

Structure from Motion (SfM) was first developed in the computer vision field by Ulman (1979). Simply stated, SfM processes the input images (minimum two) to produce a 3D point cloud (3DPC) of the field of view (FOV). The algorithm behind SfM is described in detail by Robertson & Cipolla (2009). The fundamental principles of SfM involve two main steps: feature detection and correspondence, and bundle adjustment (briefly illustrated in Fig. 1). In the first step, an algorithm called Scale Invariant Feature Transform (SIFT) is used to detect the most distinguishing features in images which are invariant to changes in scale and camera orientation and likely identifiable in other images (Lowe, 2004). Once the features are detected and matched in multiple images, the relative positions of these features can be calculated. In the second step, the locations of the features from step one are used in a bundle adjustment process (Robertson & Cipolla, 2009; Triggs *et al*., 2000) to estimate the parameters of the scene including the individual positions and orientations of the cameras, the intrinsic camera lens parameters (e.g. skew, focal length, principal point and radial distortion parameters) and derive the 3D coordinates (unit: pixel) of the features. Therefore, the accuracy of the reconstructed 3DPC improves as more features are detected.

The resulting 3DPC from the SfM process comprises the most distinctive features of the FOV and is relatively sparse which is not sufficient for data analysis. A further step, Multi View Stereo (MVS), increases the number of reconstructed points by two or three orders of magnitude and removes outliers thus producing a more detailed and accurate 3DPC (Furukawa & Ponce, 2010; James & Robson, 2012; Smith *et al*., 2016).

SfM-MVS has been used in wide range of applications such as 3D topographical surveying, monitoring glacier movement, observing and tracking lava movement and landslide displacement (Smith *et al*., 2016). James & Robson (2012) assessed the precision of SfM-MVS by comparing a 3DPC produced from the open source SfM-MVS software *Bundler* with data obtained by a laser scanner. The determined precision varied from 69-110$\mu$m for an average imaging distance of 0.7m. This suggests the ratio of precision to imaging distance was determined as approximately 1:6400 and thus the precision could therefore be improved by reducing the distance between camera and FOV. *MicMac* was chosen because of its ability to produce a high density and accurate 3DPC and it allows users to adjust the data analysis procedure to suit specific needs. Smith *et al*. (2016) reported that *MicMac* outperformed other common commercial and open source software because of its sophisticated self-calibration camera models. Galland *et al*. (2016) reported *MicMac* can produce 3DPC with a precision of approximately 50$\mu$m on elevation and horizontal displacements by using four 24 MegaPixel (MP) cameras covering a FOV of 400×400mm.

### *Limitations and requirements*

SfM-MVS relies on the feature detection and correspondence algorithm to establish the 3DPC which only works well on a FOV with good texture. In geotechnical physical experiments, natural sands have

good texture and hence are suitable for this technique. Uniform clays require artificial texture such as sand or flock at its surface to produce detailed and accurate 3DPC. In order to aid the feature matching process, two-thirds of the images should overlap.

The data points in the obtained 3DPC from SfM-MVS have their coordinates in image space (pixels) and need to be transformed into object space (in this case mm). To enable this transformation a minimum of three Ground Control Points (GCP) are required for the geo-referencing process.

Smith *et al*. (2016) reported that the SfM-MVS application is only suitable for static FOV or ones that have only very slow movements (compared with the image acquisition time) as normally only one camera moving to new locations is used to capture the images. This can be overcome by synchronising multiple cameras to capture images of the deforming FOV simultaneously to freeze the motion and minimise the reprojection errors. The solutions to tackle these requirements and limitations are now presented.

## APPARATUS DEVELOPMENT

The complete 3D imaging apparatus is presented in Fig. 2. The following sections describe the components of the apparatus in detail.

### *Cameras and lenses*

At least two images are required by SfM-MVS but more images increase the accuracy and resolution of the model as more features can be detected. Three 2MP cameras UI-5360CP-M-GL (supplied by IDS Imaging Development Systems GmbH) were used in this research (Fig. 2). The key features of these cameras are the use of a global shutter sensor and the capability to take a time sync signal. A rolling shutter sensor is not recommended as potentially, in dynamic scenes, the resulting images may not be captured at the same moment causing considerable reconstruction errors. Similarly, to eliminate any delay in image acquisition, an electrical signal was used to trigger the three cameras to capture images at the same instant. A programme, InstIm (Instant Imaging), was written to trigger the cameras to capture and save images for later analysis.

The lenses used are 8mm fixed focal length Kowa LM8JCM specifically designed for machine vision purposes with low distortion level. These short focal length lenses allow the FOV to be captured at the imaging distance of approximately 330mm.

### *Reference plate*

Even though a minimum of only three GCPs are required for the georeferencing process, a set of 59 GCPs were provided on a reference plate (Fig. 2) as more GCPs result in a more robust solution and less sensitivity to error on any one point (Smith *et al*., 2016). These GCPs are arranged towards the edge of the Region of Interest (ROI) so that the coordinate transformations are not being extrapolated. This reference plate was fabricated by a CNC machine to an accuracy of 5$\mu$m.

### *The frame*

The apparatus was designed specifically for a centrifuge modelling environment which puts significant constraints on space. The components must be relatively stiff due to the high acceleration field. The

cameras and the reference plate are securely fixed to the gantry. With this setup, the whole ROI and all 59 GCPs are visible in the three images which is beneficial for the SfM-MVS and georeferencing processes. For physical experiments at 1g, the apparatus could be more simple and straightforward to setup.

*Lighting conditions*

For imaging analysis and in order to achieve a detailed and accurate 3DPC the contrast in the images needs be good so that the maximum number of the features can be detected. Two strips of LED lights were used to ensure bright, uniform light on the FOV.

## ACCURACY AND PRECISION QUANTIFICATION

The following sections describe two sets of experiments carried out to quantify the performance of the system for measuring vertical and horizontal displacements.

*Vertical direction*

Fig. 2 illustrates the setup used to quantify the performance of the measurement system in the vertical direction by comparing the measured change in elevation with the true value. The measured ROI is a surface plate which has its elevation determined relative to the reference plate. The area of the ROI is 300×130mm. The actual change in the elevation of the surface plate, Uz, is realised by placing slip gauges of thickness Uz between the reference and surface plates. Six 3DPCs of the measured ROI were reconstructed representing the changes in vertical direction Uz of 0mm (reference 3DPC), 2.540mm, 5.105mm, 10.160mm, 15.240mm and 25.400mm. A typical accuracy calculation is illustrated in Fig. 3. The reconstructed 3D surfaces were divided into 10mm cells. The elevation of cell $i$, $Z_i$, is the average of the elevations of all the points within that cell. Fig. 4 shows accuracy histograms for the first four elevation increments respectively. The accuracy and precision of each of these four increments was found to be better than 50μm. For the large change in elevation Uz = 25.400mm, some parts of the ROI were out of focus, which may explain the observed reduction in accuracy and the results are not presented here.

*Horizontal directions*

Four experiments have been conducted using the controlled movement of a sliding bed (Fig. 5) to realise horizontal displacements. In each experiment, the sliding bed was moved by 1mm in either the X or Y direction.

The *'master image'* (image taken by the central camera) has been undistorted and unwarped (Fig. 6) prior to conventional 2D PIV being carried out on the new set of images to measure the horizontal displacements. Details on 2D PIV principles and applications in centrifuge modelling can be found in White *et al.* (2003) and Nadimi *et al.* (2016). 2D PIV analysis on the rectified master images show standard deviations of less than 35μm. The accuracy histograms from four experiments are shown in Fig. 7.

Fig. 6 gives a flow chart showing the process of coupling the 2D PIV analysis with the 3D point clouds obtained from SfM-MVS to determine 3D displacements. Firstly, a mesh of cells on the transformed image was generated for 2D PIV tracking purposes. The XY coordinates of these cells in the sequential images were then obtained. The transformed images and 3D point clouds are in the same Cartesian coordinate system as they use the same reference plate for transformation. The Z coordinate of a cell in the 2D PIV analysis is derived by averaging the Z coordinates of points which lie within that cell in the corresponding 3D point cloud. As a consequence, XYZ coordinates of cells are obtained and the 3D displacements can then be derived. The reliability and repeatability of the 3D imaging system is confirmed by the consistent accuracy and precision achieved in two sets of performance quantification experiments.

The performance of the reported 3D Imaging System relies on 2D PIV and the SfM-MVS process. Both of these procedures require a set of GCPs for transformation which should ideally be distributed evenly in the ROI. However, having GCPs in the middle of the ROI would have obstructed the scene and reduced the system performance. Other errors come from the SIFT algorithm and bundle adjustment. Higher resolution cameras will increase the number of features detected and hence improve the system performance.

## EXAMPLE APPLICATION

Fig. 8 shows a three dimensional centrifuge test model simulating ground movements at a tunnel heading as the tunnel support pressure is reduced. Artificial texture was created by spraying Fraction E Leighton Buzzard Sand onto a previously applied plastic coating (which prevents moisture loss at the model top surface). The ROI is 390×175mm. Details of the testing procedure of similar models can be found in Le & Taylor (2016). The 3D imaging system and PIV were used to measure the soil deformations of the top surface and the front face of the model respectively. Results from the new system can be compared with those from conventional PIV by inspecting soil at the front surface (shown in Fig. 8).

Fig. 9 and 10 compare the vertical and horizontal displacements of those soil elements. The results show the maximum difference in the displacements measured by the 3D imaging system and PIV are 33μm and 35μm in horizontal and vertical directions respectively.

Finally, by combining the horizontal and vertical displacements determined by the analysis techniques described above and illustrated in Fig. 6, a map of 3D displacement vectors can be obtained for the entire surface (Fig. 11).

## CONCLUSION

With the newly developed 3D imaging system using SfM-MVS combined with conventional 2D PIV, three dimensional displacements of a moving soil model surface can be measured to an accuracy of

50μm (1/10,000th of the FOV) and 35μm (1/14,200th of the FOV) in vertical and horizontal directions respectively.

ACKNOWLEDGEMENTS

The first author would like to express sincere thanks to Vietnam government for funding his doctoral scholarship. The second author acknowledges City University London for his doctoral scholarship.

REFERENCE

Furukawa, Y., & Ponce, J. (2010). Accurate, dense, and robust multiview stereopsis. *IEEE Trans. Pattern Anal. Mach. Intell.* **32**, 1362-1376.

Galland, O., Bertelsen, H. S., Guldstrand, F., Girod, L., Johannessen, R. F., Bjugger, F., Burchardt, S. & Mair, K. (2016). Application of open-source photogrammetric software MicMac for monitoring surface deformation in laboratory models. *J. Geophys. Res. Solid Earth* **121**, 2852–2872.

James, M. R. & Robson, S. (2012). Straightforward reconstruction of 3D surfaces and topography with a camera: Accuracy and geoscience application. *Journal of geophysical research* **117**, F03017.

Le, B.T. & Taylor, R.N. (2016). A study on the reinforcing capabilities of Forepoling Umbrella System in urban tunnelling. *Proceeding of the 3rd European Conference on Physical Modelling in Geotechnics*, Eurofuge2016. Nantes, France.

Lowe, D.G. (2004). Distinctive image features from scale-invariant keypoints. *International Journal of Computer Vision* **60**, 91-110.

Nadimi, S., Divall, S., Fonseca, J., Goodey, R. & Taylor, R.N. (2016). An addendum for particle image velocimetry in centrifuge modelling. *Proceeding of the 3rd European Conference on Physical Modelling in Geotechnics*, Eurofuge2016. Nantes, France.

Robertson, D.P. & Cipolla, R. (2009). Structure from motion. In: Varga, M., (Ed.), *Practical Image Processing and Computer Vision.* John Wiley and Sons Ltd., New York.

Smith, M.W., Carrivick, J. & Quincey, D. (2016). Structure from motion photogrammetry in physical geography. *Progress in Physical Geography* **40**: 247-275.

Taylor, R.N., Grant. R., Robson, S. & Kuwano, J. (1998). An image analysis system for determining plane and 3D dis-placement in soil models. *Proceeding of the International Conference on Centrifuge Modelling*, Centrifuge 98, Tokyo, Japan.

Triggs, W., McLauchlan, P., Hartley, R. & Fitzgibbon, A. (2000). Bundle adjustment – A modern synthesis. In W. Triggs, A. Zisserman, and R Szeliski, editors, *Vision Algorithms: Theory and Practice*, LNCS, pages 298–375. Springer Verlag.

Ullman, S. (1979). The interpretation of structure from motion, *Proceedings of The Royal Society of London Series B Biological Sciences* **203**, 405-426.

White, D. J., Take, W. A. & Bolton, M. D. (2003). Soil deformation measurement using particle image velocimetry (PIV) and photogrammetry. *Géotechnique* **53**, No. 7, 619–631.

LIST OF FIGURES

Fig. 1. Structure from Motion (SfM) principle.

Fig. 2. 3D topography apparatus.

Fig. 3. Determination of vertical displacement accuracy on reconstructed 3DPC of measured surfaces when Uz = 0mm (reference surface) and Uz = 25.4mm.

Fig. 4. Accuracy histograms in four elevation increments. The total number of cells is 390.

Fig. 5. Experiment set up to quantify horizontal displacement measurement accuracy.

Fig. 6. Schematic of 2D PIV analysis combined with SfM-MVS to obtain 3D displacements.

Fig. 7. Accuracy histograms in four horizontal displacements. The total number of cells is 336.

Fig. 8. Example application: Three dimensional centrifuge model simulating tunnel construction.

Fig. 9. Comparison on the vertical surface settlement above the tunnel face measured by 3D imaging system and 2D PIV (The measured locations are depicted in Fig. 8).

Fig. 10. Comparison on horizontal displacements measured by 3D imaging system and 2D PIV when tunnel support pressure was reduced from 206 to 106kPa. (The measured areas are depicted in Fig. 8).

Fig. 11. (a) 3D displacement vectors on the top model surface when the tunnel support pressure was reduced from 206 to 106kPa.

(b) Corresponding map of vertical settlement magnitude.

(c) Model tunnel position with respect to the map of vertical settlement.

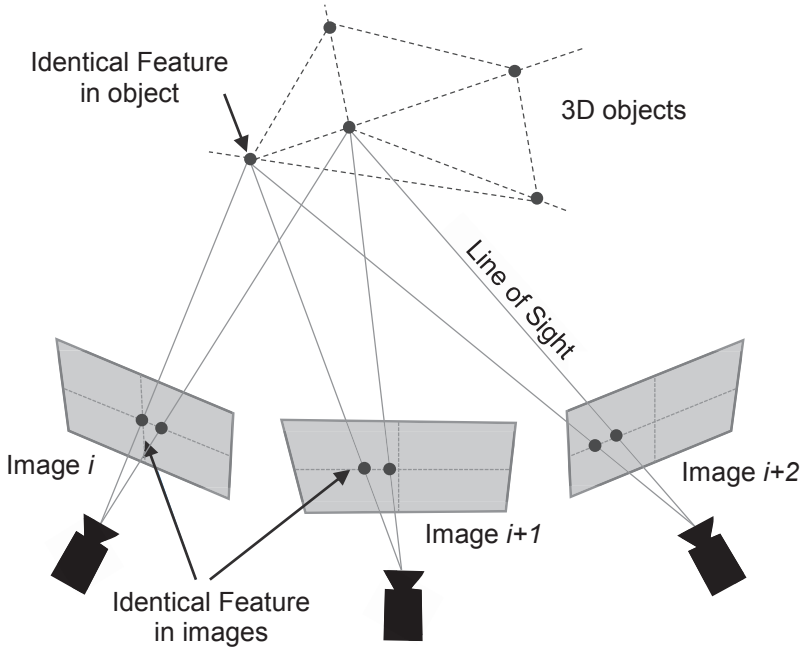


Fig. 1. Structure from Motion (SfM) principle.

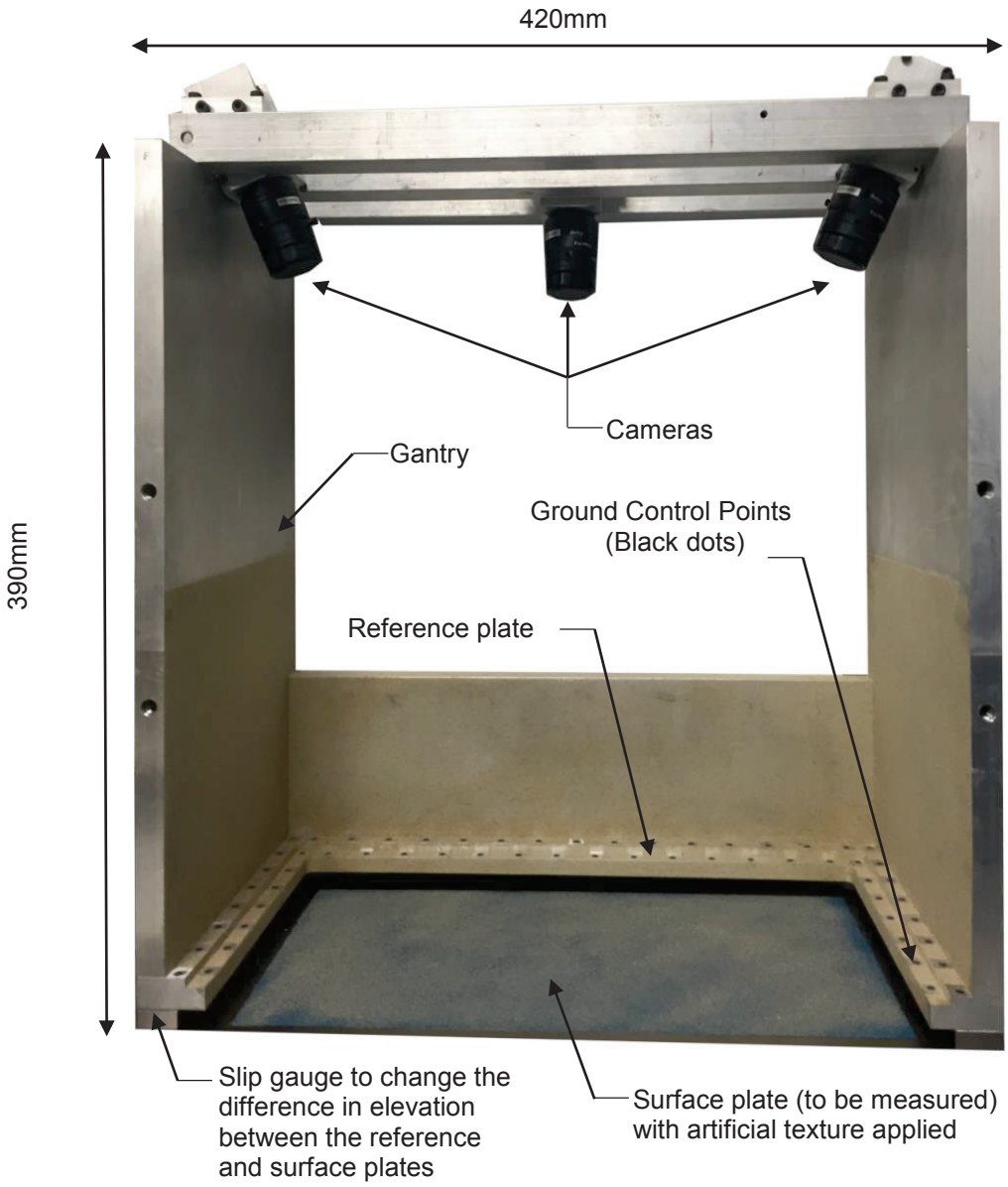


Fig. 2. 3D topography apparatus.

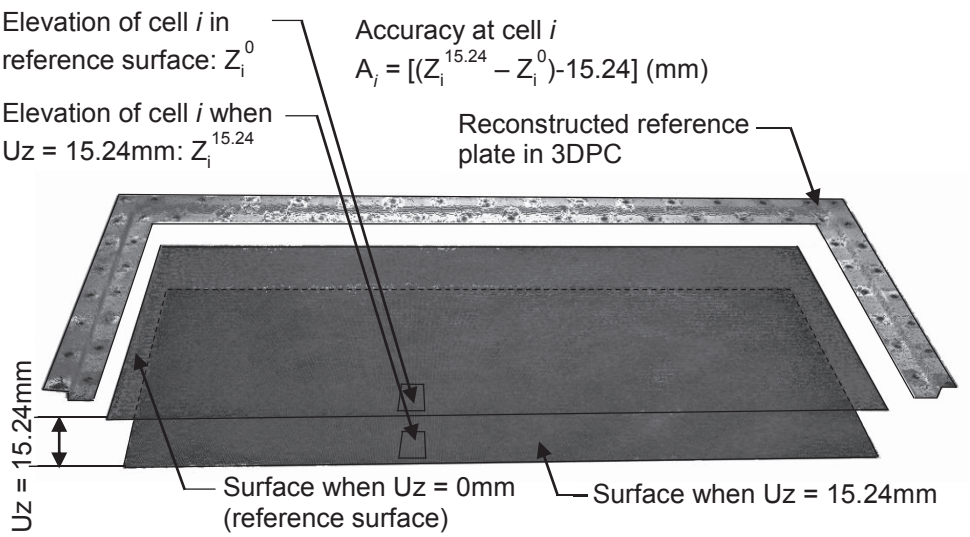


Fig. 3. Determination of vertical displacement accuracy on reconstructed 3DPC of measured surfaces when Uz = 0mm (reference surface) and Uz = 15.24mm.

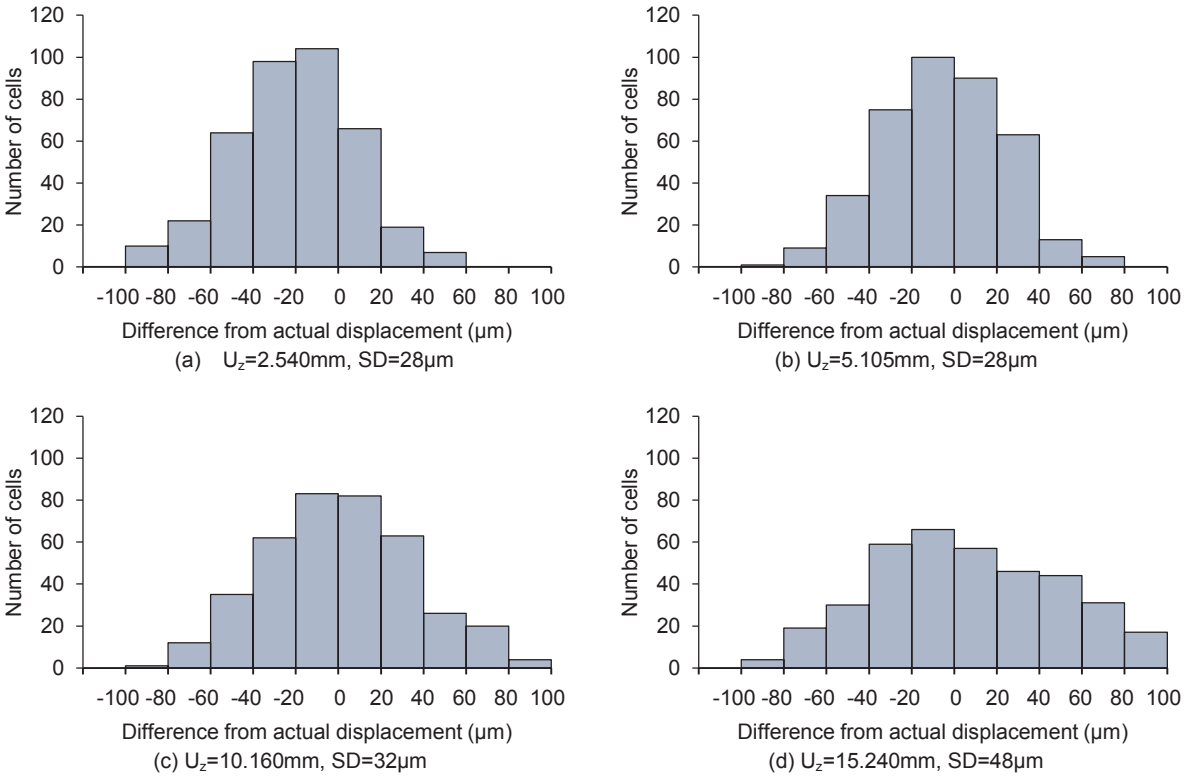


Fig. 4. Accuracy histograms in four elevation increments. The total number of cells is 390.

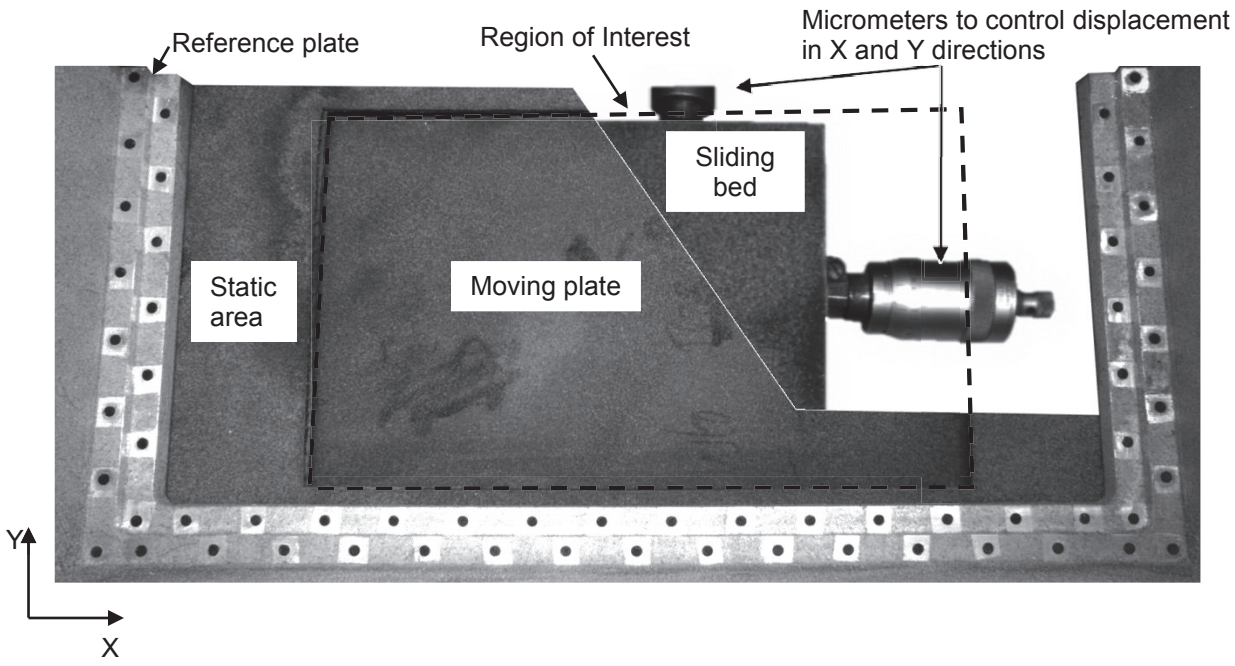


Fig. 5. Experiment set up to quantify horizontal displacement measurement accuracy.

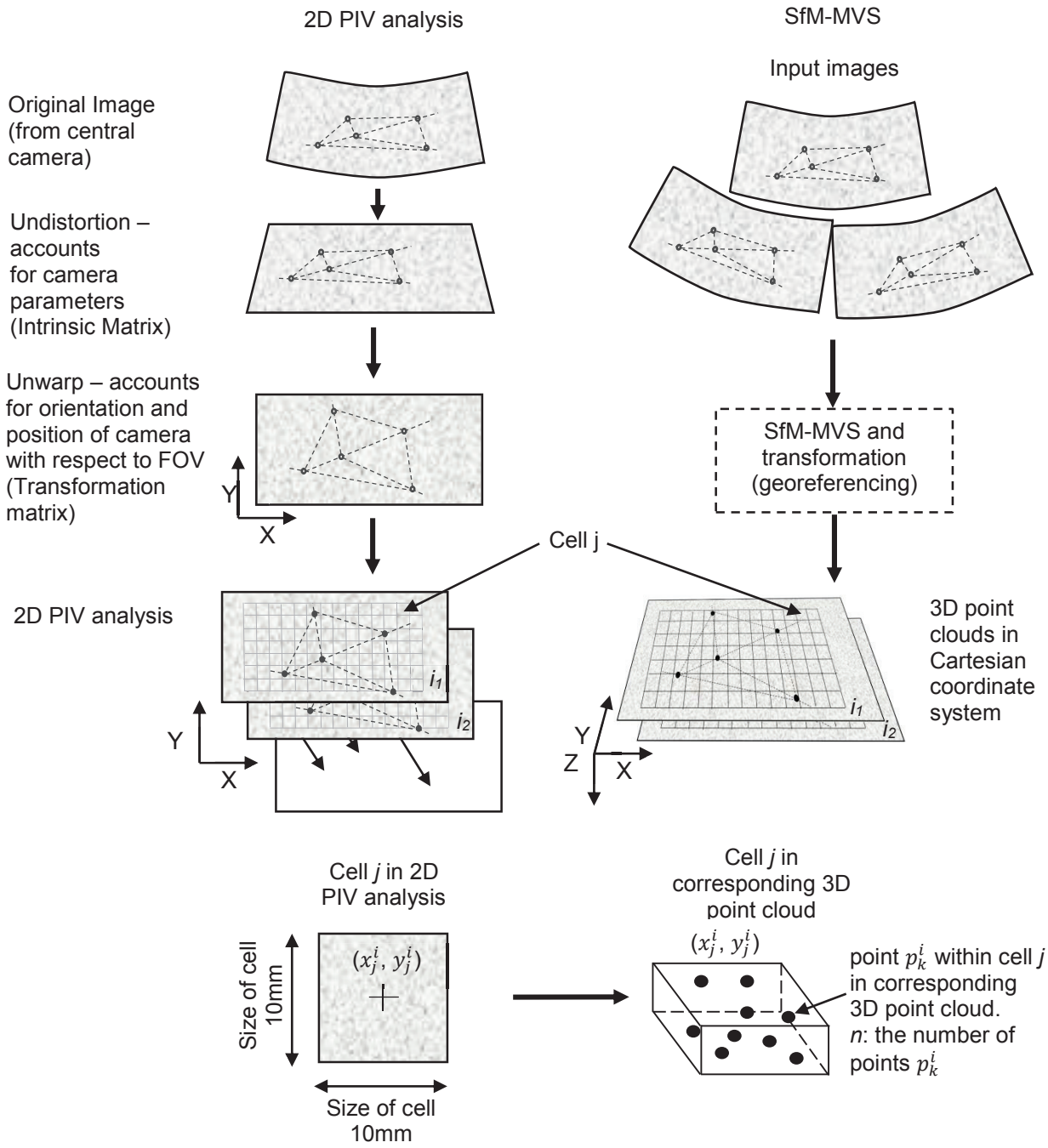


Fig. 6. Schematic of 2D PIV analysis combined with SfM-MVS to obtain 3D displacements (not to scale).

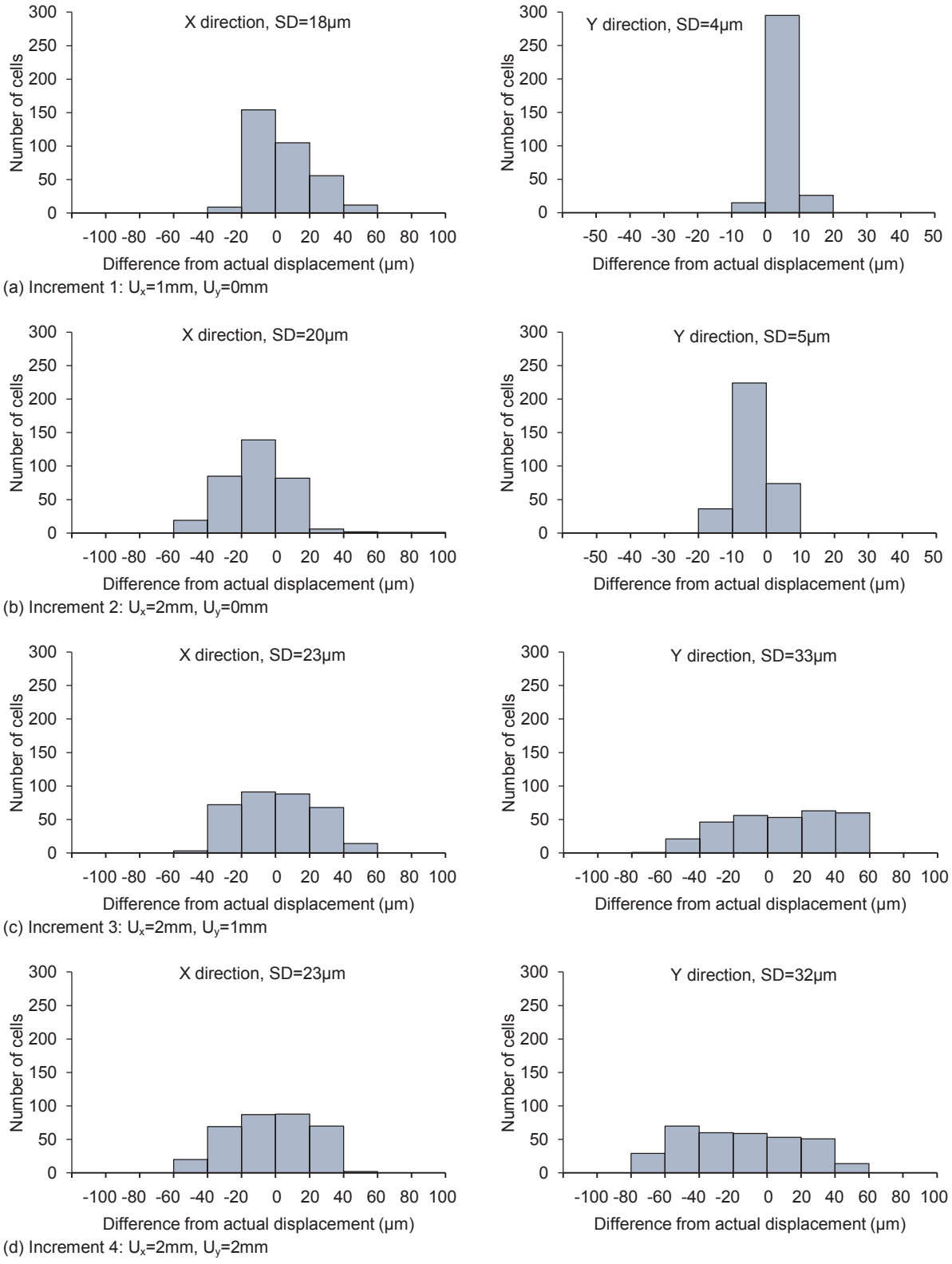


(a) Increment 1: $U_x$=1mm, $U_y$=0mm

(b) Increment 2: $U_x$=2mm, $U_y$=0mm

(c) Increment 3: $U_x$=2mm, $U_y$=1mm

(d) Increment 4: $U_x$=2mm, $U_y$=2mm

Fig. 7. Accuracy histograms in four horizontal displacements. The total number of cells is 336.

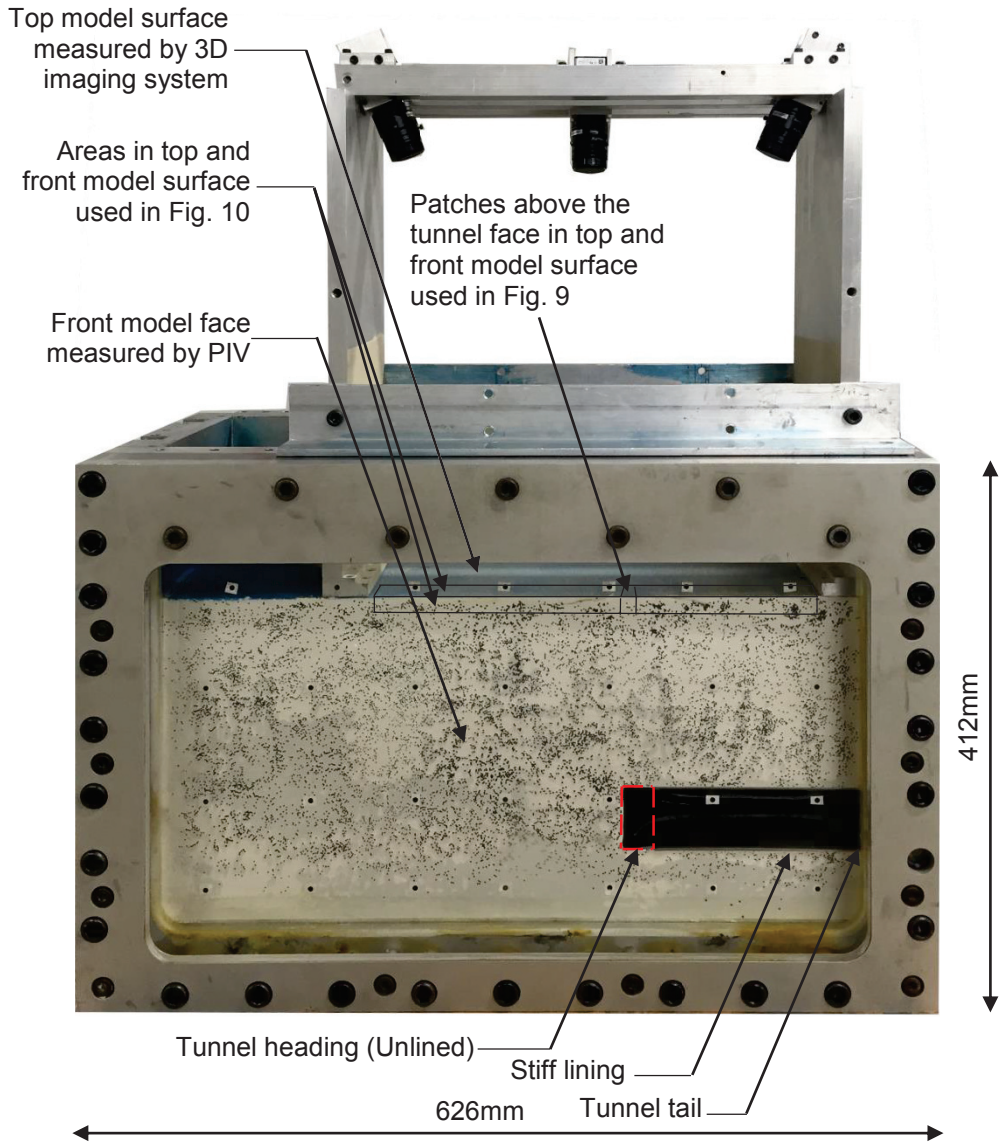


Fig. 8. Example application: Three dimensional centrifuge model simulating tunnel construction.

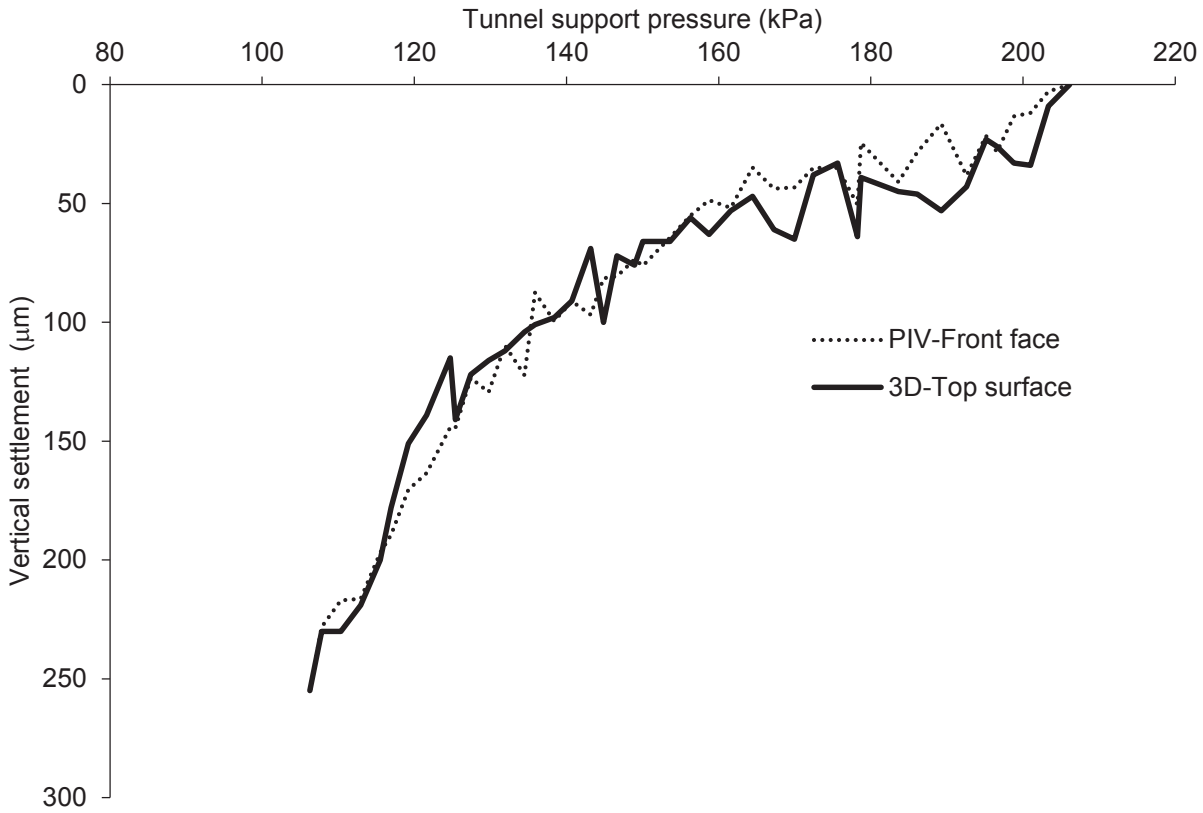


Fig. 9. Comparison on the vertical surface settlement above the tunnel face measured by 3D imaging system and 2D PIV (The measured locations are depicted in Fig. 8).

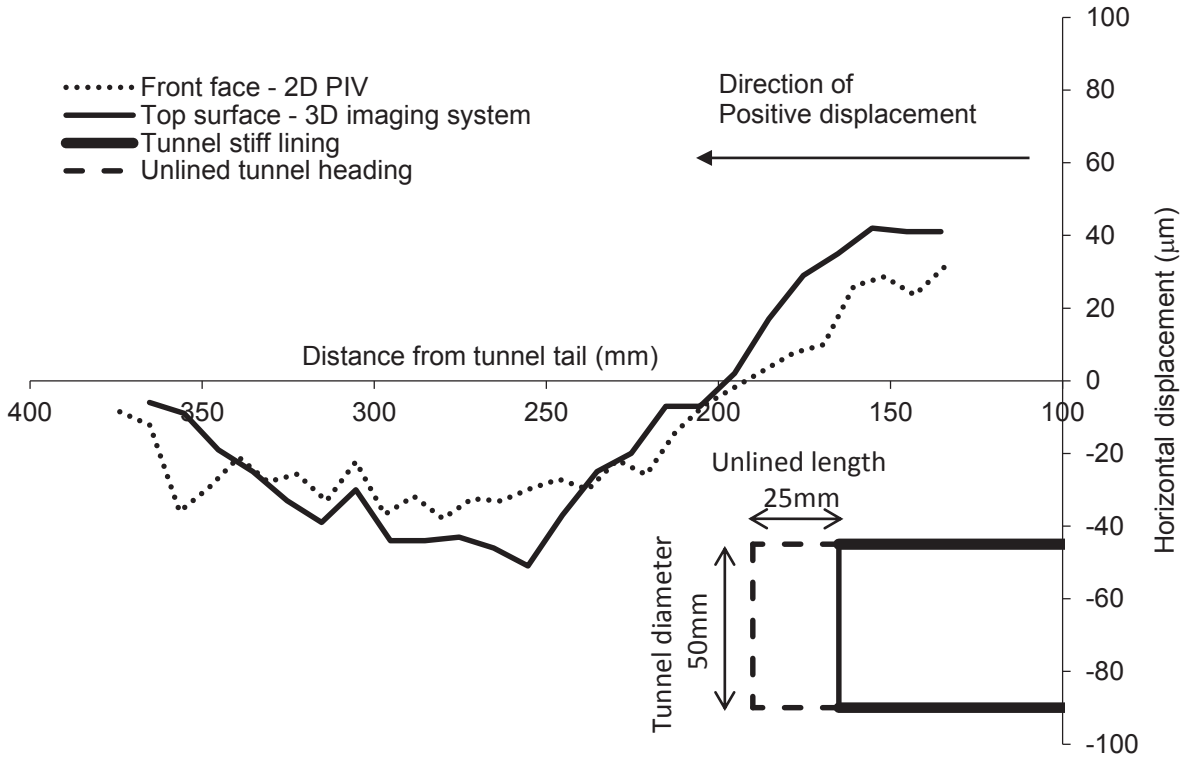


Fig. 10. Comparison on horizontal displacements measured by 3D imaging system and 2D PIV when tunnel support pressure was reduced from 206 to 106kPa. (The measured areas are depicted in Fig. 8).

Fig. 11

Click here to download Figure Fig. 11.pptx

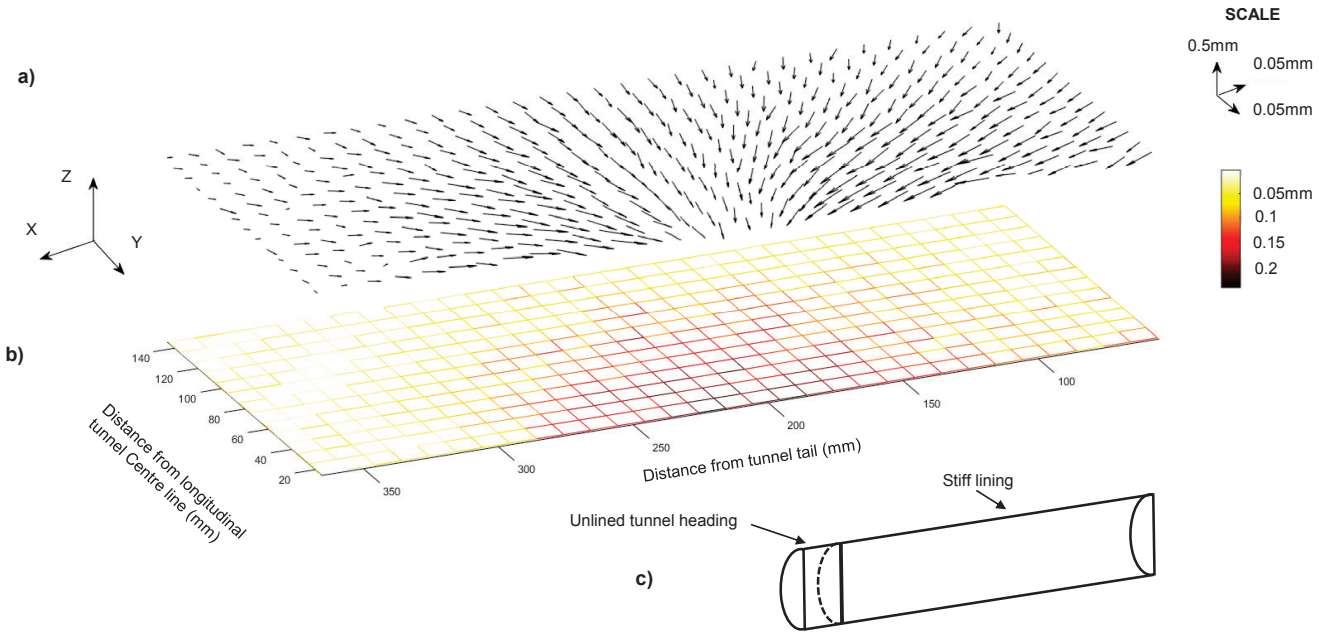


Fig. 11. (a) 3D displacement vectors on the top model surface when the tunnel support pressure was reduced from 206 to 106kPa.
(b) Corresponding map of vertical settlement magnitude.
(c) Model tunnel position with respect to the map of vertical settlement.